Pressure Fluctuations as a Diagnostic Tool for Fluidized Beds

DOE/PC/94210--T6

Technical Progress Report for the Period
July 1, 1996 - September 30, 1996

Principal Investigator: Robert C. Brown
Research Assistant: Ethan Brue

Iowa State University
Ames, IA 50011

Work Performed Under Grant
No. DE-FG22-94PC94210

Date Transmitted: October 10, 1996

Prepared for: U.S. Department of Energy
Pittsburgh Energy Technology Center
Pittsburgh, PA

Pressure Fluctuations as a Diagnostic Tool for Fluidized Beds

Technical Progress Report for the Period
July 1, 1996 - September 30, 1996

Principal Investigator: Robert C. Brown
Research Assistant: Ethan Brue
Iowa State University
Ames, IA 50011

Abstract

By studying pressure fluctuations using a system identification approach, it is hypothesized that CFB pressure fluctuations are indicative of CFB hydrodynamics in two ways. First, the frequency phenomenon that is observed in the lower regions of the CFB under conditions of high solids loading is the result of lower dense bed voidage oscillations. Our results suggest that a surface wave phenomena inversely proportional to the square root of the bed diameter is also be observed in CFB pressure fluctuations under most conditions.

By matching revised similitude parameters between two CFBs a number of conclusions can be drawn. First, spectral analysis of pressure fluctuations, if properly applied, can be used to verify that similitude has been achieved. To do this, not only must the Bode plot characteristics important for hydrodynamics be identified, but the pressure fluctuation structure at all elevations of the CFB must be similar. The set of similitude parameters defined by Glicksman is not sufficient to establish hydrodynamic similitude. The solids flux as typically measured in the downcomer does not contain information on the solids hold-up in the riser, or the amount of solids that progress downwards in the annulus rather than exit the riser. It is better to use the total mass contained in the riser as the important "solids" parameter for the establishment of similitude, rather than the solids flux. This measurement can be made more accurately, monitored continuously, and is a much simpler measurement to perform in most CFB systems. Even with this new set of dimensionless parameters, the differences in the coefficient of restitution of particle/bed collisions may make a significant difference in the CFB hydrodynamics. The effects of particle collisions with the riser top-plate must be considered in similitude studies.

DISCLAIMER

Pressure Fluctuations as a Diagnostic Tool for Fluidized Beds

Robert C. Brown and Ethan Brue

Objective

The purpose of this project is to investigate the origin of pressure fluctuations in fluidized bed systems. The study will asses the potential for using pressure fluctuations as an indicator of fluidized bed hydrodynamics in both laboratory scale cold-models and industrial scale boilers.

Progress

Experimental Set-up

CFB Models

This study was performed in two geometrically similar cold-flow CFBs, illustrated in Figure 1. The riser of the larger unit (prototype) is 10.2 cm in diameter and 3.00 m tall. This unit is fluidized with 0.2, 0.3, and 0.4 mm diameter glass beads. Pressure taps are located at 25.4 cm intervals along the riser, with two additional pressure taps spaced evenly between the first 25.4 cm interval. Each pressure tap is threaded into the CFB so that the tap is flush with the inner wall. The riser, cyclone, and L-valve of both circulating fluidized beds are constructed of aluminum to reduce electrostatic effects. The downcomer and solids flux meter are constructed of Plexiglas to allow visual observation of bed operation. The 10.2 cm diameter CFB has two small Plexiglas sections in the riser to observe solids circulation. This large CFB is designed to be operated only at atmospheric pressure, using air as the fluidizing gas. The smaller unit is a one-half scale model of the larger unit with an inside diameter of 5.08 cm and a height of 1.50 m. The smaller CFB (model) is fluidized with 0.1, 0.15, and 0.2 mm diameter steel shot, for the purpose of conducting hydrodynamic similitude studies between the two beds. Since the fluidizing gas density must be greater in the small bed in order to achieve similitude, it is fluidized with pressurized air (0-200 kPa gage).

Solids flux measurement

Since the accurate measurement of solids flux is very important for similitude studies, a meter was constructed that, when activated, would capture particles as they exited the cyclone. A schematic of this solids flux meter is shown in Figure 2. The time it takes for this meter to fill is recorded and converted to a solids flux in kg/m²s. The design of this meter involved a trade-off. If the meter was constructed too small, the time at which it filled would be to short for high accuracy measurements. If it was built too large, the particles removed by the meter would significantly reduce the height of the particles in the L-valve. This change in downcomer bed height reduces the solids circulation rate of the system during measurement. Designing a valve to release the particles from the meter after measurement proved to be difficult. In the end, a simple plug suspended from a fine nylon line that extended down through the top of the cyclone worked surprisingly well. The meter measured the solids flux with an overall accuracy of around ± 10%, which is good considering the variation in the solids flux inherent in bed operation.

Background

CFB Similitude

For CFB hydrodynamics, Glicksman [15] adds an additional independent variable, Gs [kg/m²s], to the list previously described for bubbling fluidized bed systems. Using the Buckingham Pi theorem, the full set of independent dimensionless parameters for circulating fluidized beds is summarized as follows:

$$Fr = \frac{U^2}{g \cdot d_p} \qquad \frac{H}{d_p} \qquad \frac{D}{d_p} \qquad \frac{\rho_g}{\rho_s} \qquad \mathrm{Re}_p = \frac{\rho_g \cdot U \cdot d_p}{\mu} \qquad \frac{Gs}{\rho_s \cdot U}$$

As discussed in previous reports, the reactor loading or total mass of particles in the entire CFB system is another independent variable that must be considered in CFB systems that use L-valves. Under identical conditions, changing the reactor loading will significantly change the resulting axial voidage profile. This additional non-dimensional reactor loading

variable was matched in this similitude study. The full set of CFB dimensionless parameters used in this study is:

$$Fr = \frac{U^2}{g \cdot d_p} \qquad \frac{H}{d_p} \qquad \frac{D}{d_p} \qquad \frac{\rho_g}{\rho_s} \qquad \mathrm{Re}_p = \frac{\rho_g \cdot U \cdot d_p}{\mu} \qquad \frac{Gs}{\rho_s \cdot U} \qquad \frac{M}{\rho_s \cdot D^3}$$

where M is the total mass of particles within the CFB system.

Results and Discussion

Fast Fluidization Fluctuations - General characteristics

Two predominant phenomena are observed in the frequency spectrum of fast fluidization systems. Figures 3-5 show typical CFB Bode plots under different operating conditions. Under relatively dilute conditions (and in the upper regions of the bed) the surface wave phenomenon appears along with its first harmonic in the spectrum (see Figure 3). In the transition from dilute to dense conditions, the Bode plot of fluctuations appears highly damped as shown in Figure 4 (i.e. no distinct peaks are observed in the pressure dynamics). Under the dense conditions shown in Figure 5, the voidage wave frequency is evident in the Bode plot. This voidage wave phenomenon is most dominant when fluctuations are measured at low elevations in the bed (5-10 % bed height). The CFB Bode plots under all conditions exhibit a final asymptotic slope of -40 dB/decade.

Discussion of voidage wave phenomenon in CFBs

By observing pressure fluctuations throughout the transition from bubbling to turbulent to fast fluidization, it is evident that the voidage wave phenomenon is present in all three regimes. This phenomenon originates from the lower dense regions of the CFB. It appears only when a lower dense bed has been established (i.e. the axial voidage profile shows decreasing voidage at low bed heights). It is also most dominantly sensed at the lower elevations of the CFB. Figure 6 shows how voidage waves are manifest in the CFB Bode plots of fluctuations measured at different elevations. Secondly, in addition to the observation of this phenomena throughout bubbling, turbulent, and fast fluidization regimes, the frequency

of this phenomena can be predicted from the modified-Hiby model proposed for bubbling fluidized beds. The height of the lower dense bed can be estimated from the axial voidage profiles to be between 10-20 cm (in the 10.2 cm diameter CFB model). The theory for voidage oscillations under turbulent conditions predicts that this frequency should appear between 2-3 Hz. All Bode plots of lower dense bed pressure fluctuations confirm this.

As expected, this voidage wave also exhibits an inverse square root dependence on dense bed height. When the two CFB models are operated such that similar axial voidage profiles are attained, the lower dense bed height in the large CFB will be twice the height of the small CFB dense bed. Consequently, the lower dense bed frequency in the model CFB appears at a frequency that is 1.4 (or $2^{1/2}$) times the frequency that is observed in the prototype CFB. This is shown conclusively in the results of the similitude study that follow. This result suggests that pressure fluctuation measurements at one location could be used as an indicator of the height of the lower dense region in a CFB

Discussion of surface wave frequency phenomena in CFBs

As seen in the transition regime, surface waves begins to appear in the high velocity turbulent regime prior to fast fluidization. This suggests that this phenomena is associated with the behavior of particles leaving and returning to the dense bed surface, rather than a phenomena associated with the structural CFB height.

Visual observations in circulating fluidized beds and turbulent beds (as they approach fast fluidization) show clusters of solids leaving the dense bed surface at approximately 1 Hz, which corresponds to the frequency peaks observed in the Bode plots. Similar to the transition regime, this frequency of sloshing/cluster propagation originating at the lower dense region of the CFB is hypothesized to be governed by a surface wave phenomena. It appears that this frequency is inversely proportional to the square root of the bed diameter, which further supports the hypothesis of pressure fluctuations governed by a deep wave phenomena.

Summary of CFB pressure fluctuations

CFB pressure fluctuations are indicative of CFB hydrodynamics in two ways. First, the frequency phenomenon that is observed in the lower regions of the CFB under conditions of high solids loading is the result of lower dense bed voidage oscillations as observed in bubbling and turbulent beds also. Our results suggest that a surface wave phenomena inversely proportional to the square root of the bed diameter is also be observed in CFB pressure fluctuations under most conditions. Knowing how pressure fluctuations reflect CFB hydrodynamics, it is possible to use the analysis of pressure fluctuations to validate proposed similitude parameters.

Investigation of CFB similitude parameters

The results of the CFB similitude study are summarized in Table 1. In Table 1 the degree of similarity between the hydrodynamics in the model and prototype CFB is presented. Under these proposed conditions of similitude, a number of characteristics can be noted. The Bode plot profiles in the upper bed (75% bed height) match relatively well in the model and prototype CFB under most conditions. This occurs even when the axial voidage profiles do not match well. This is to be expected from the present understanding of the surface wave phenomenon, which dominates in the upper CFB elevations. The surface wave phenomenon is primarily a function of bed diameter and is not expected to vary with changing operating conditions. The surface wave (dimensionless) frequency will match in two CFBs as long as the bed diameters are scaled properly. Consequently, it cannot be assumed in similitude studies that pressure fluctuations in the upper regions can by themselves verify similitude relations. Upper bed fluctuations must be used in conjunction with lower bed fluctuations and axial voidage profiles before any valid conclusions regarding CFB similitude can be made.

In contrast to upper CFB Bode plots, the lower dense bed fluctuations and axial voidage profiles are rarely similar in prototype and model under Glicksman's conditions of similitude. The model shows a significantly higher voidage in the lower bed than the prototype. The voidage wave frequency in the prototype and model CFB rarely exhibit similar

dimensionless frequency and damping. Only under dilute operating conditions were approximately similar hydrodynamics occasionally observed.

It is also important to observe that the matching of Glicksman's similitude parameters does not guarantee that choking conditions in one bed will yield choking conditions in the other. There are three experiments in the model (shown in Table 1) that could not be duplicated in the prototype due to conditions of complete choking under the prescribed similitude parameters.

It is hypothesized from these experiments that solids flux is not an appropriate independent variable for the establishing of similitude. Representing a measure of the rate of particles leaving the riser, it is not fundamentally an indicator of the total amount of solids suspended in the riser, which is more important for similitude studies.

An alternative to dimensionless solids flux is suggested by these results. Dimensionless solids loading in the riser was substituted for dimensionless solids flux in the experiments illustrated in Figures 7-16. This was done by maintaining the appropriate level of solids (L_v) in the CFB downcomer. The full set of dimensionless similitude parameters used in this approach is:

$$Fr = \frac{U^2}{g \cdot d_p} \qquad \frac{H}{d_p} \qquad \frac{D}{d_p} \qquad \frac{\rho_g}{\rho_s} \qquad \mathrm{Re}_p = \frac{\rho_g \cdot U \cdot d_p}{\mu} \qquad \frac{M}{\rho_s \cdot D^3} \qquad \frac{L_v}{D}$$

The pressure fluctuation Bode plots and the axial voidage profiles match very well when this full set of parameters is matched. In spite of these hydrodynamic similarities, there is one obvious difference between the conditions in the two cases. The dimensionless solids flux (now used as a dependent parameter) is over 50% greater in the model than the prototype. It was hypothesized that this may be the result of differences in the elasticity of the solids in the riser; changing the dynamics of particle/particle or particle/bed collisions.

Since the predominant collisions in the riser occur between particles and the riser top-plate, differences between the steel shot/aluminum top-plate (model) collisions and the glass bead/Plexiglas top-plate (prototype) collisions were investigated. By measuring the rebound height of steel and glass beads, the coefficients of restitution were estimated:

$$e = \sqrt{\frac{h_r}{H_d}}$$

where H_d is the drop height and h_r is the rebound height. The resulting coefficient of restitution of glass/Plexiglas collision is over 50% higher than the coefficient of restitution of steel/aluminum collision. This being the case, the glass particles in the large CFB model are more likely to rebound off the top-plate and back down into the riser, rather than exiting the riser to the cyclone. As a result, the internal recycle rate of steel shot will be much higher, yielding a higher solids flux in the model reactor. The axial voidage profiles in Figures 7 and 12 support this hypothesis by showing a slightly denser upper region in the prototype.

To definitively support this hypothesis that the top-plate collision strongly affects the measured solids flux, 26" and 13" extensions were added to the large and small CFBs respectively. These extensions allowed particles to progress beyond the riser exit, and change direction, without contacting the riser top-plate. The results of this experiment presented in Figures 17-21 confirms that the coefficient of restitution of particle/bed collisions is an important consideration in similitude studies. In this experiment, the dimensionless solids flux matches exactly in both beds, in addition to pressure fluctuations and axial voidage profiles. Complete hydrodynamic similitude was achieved in this test.

A number of conclusions can be drawn from this CFB similitude study. First, spectral analysis of pressure fluctuations, if properly applied, can be used to verify that similitude has been achieved. To do this, not only must the Bode plot characteristics important for hydrodynamics be identified, but the pressure fluctuation structure at all elevations of the CFB must be similar. The set of similitude parameters defined by Glicksman is not sufficient to establish hydrodynamic similitude. The solids flux as typically measured in the downcomer does not contain information on the solids hold-up in the riser, or the amount of solids that progress downwards in the annulus rather than exit the riser. It is better to use the total mass contained in the riser (using a measurement such as L_v) as the important "solids" parameter for the establishment of similitude, rather than the solids flux. This measurement of L_v can be made more accurately, monitored continuously, and is a much simpler measurement to

perform in most CFB systems. Even with this new set of dimensionless parameters, the differences in the coefficient of restitution of particle/bed collisions may make a significant difference in the CFB hydrodynamics. The effects of particle collisions with the riser top-plate must be considered in similitude studies.

Future Work

Future work will focus on further confirming the hypothesized mechanisms that govern fluidized bed pressure fluctuations. More work will be done in developing an appropriate set of similitude parameters for CFB systems.

A – 2.0" ID x 1/4"W Plexiglas
B – 2.0" ID x 1/4"W Aluminum
C – 2.0"x 1.0" – 1/8"W Aluminum
D – Aluminum Cyclone
E – Plexiglas solids flux meter
F – 1.25" ID x 1/8"W Plexiglas

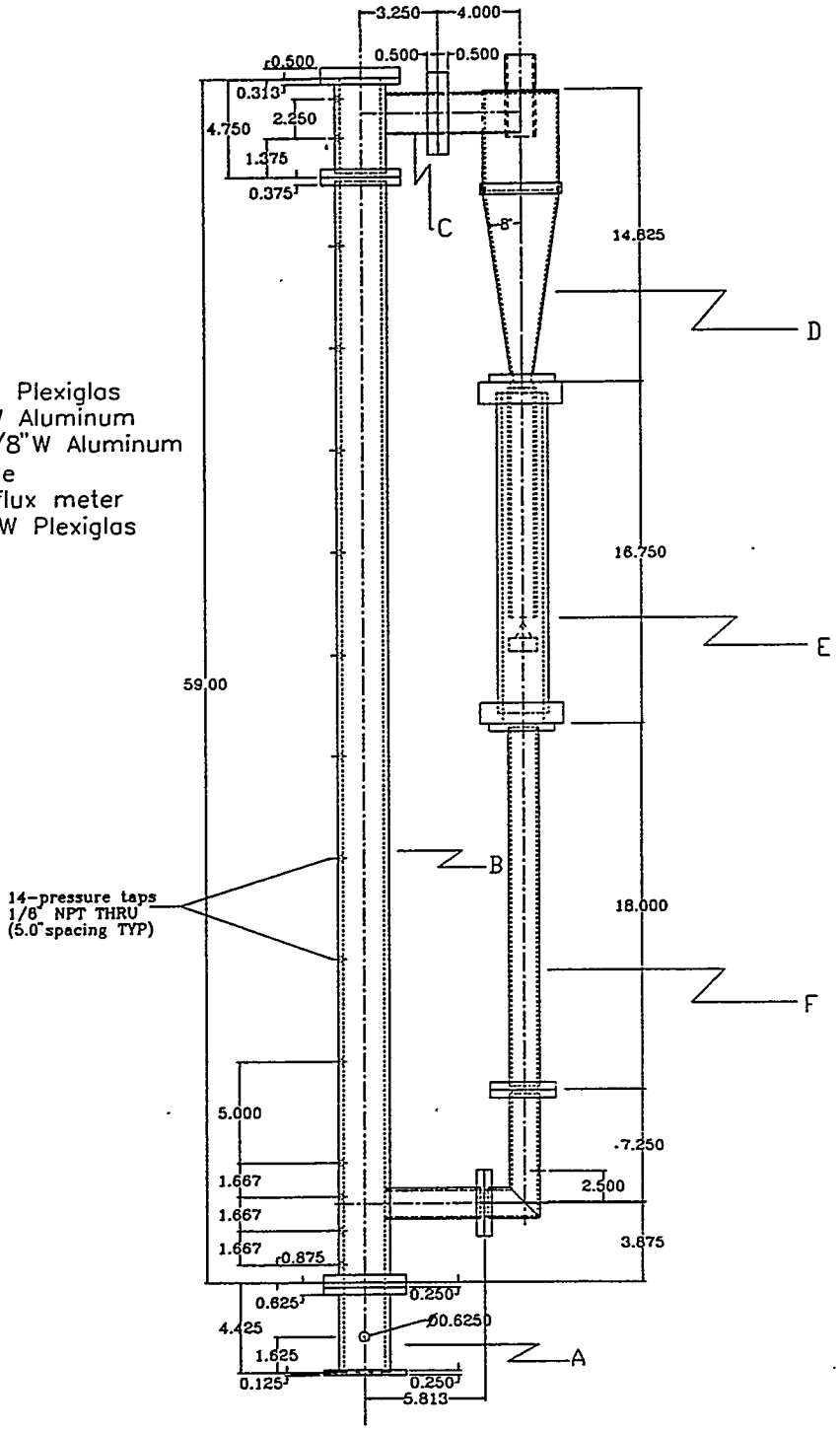

- Dimensions are given for model CFB in inches

(Dimensions for prototype CFB are twice those given above)

Figure 1: Cold-flow model CFB

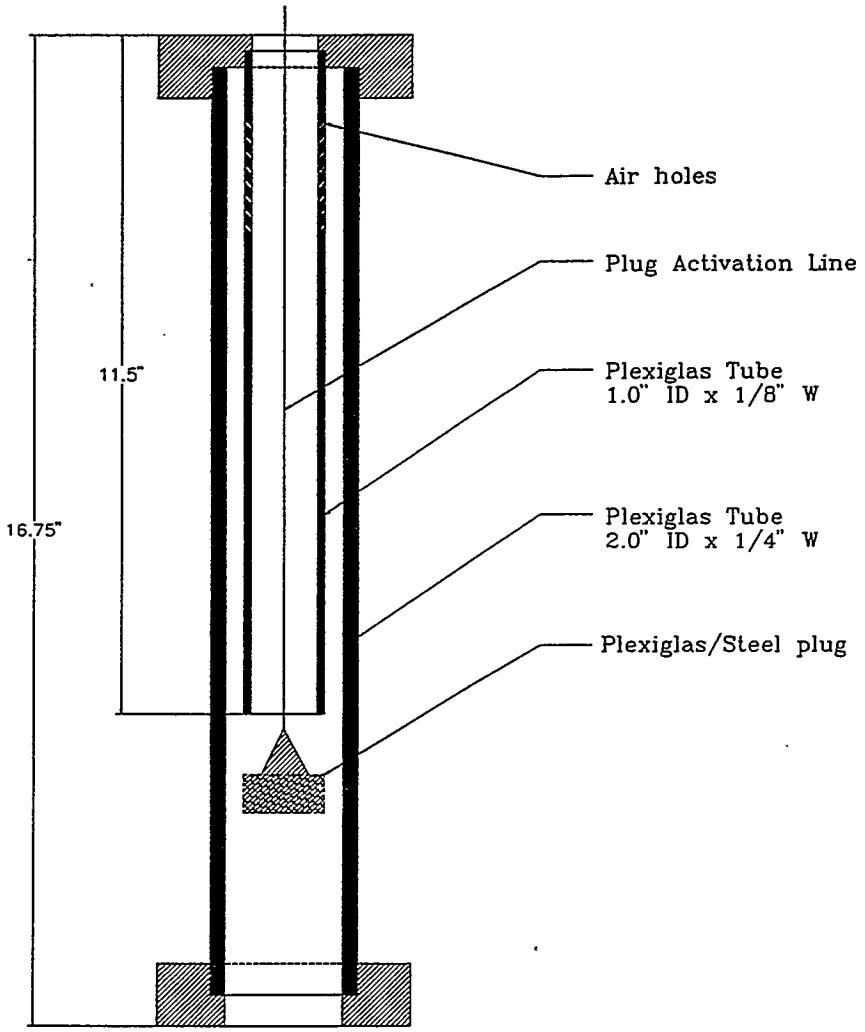

Dimensions given are for the small CFB solids flux meter

Figure 2: Solids flux meter

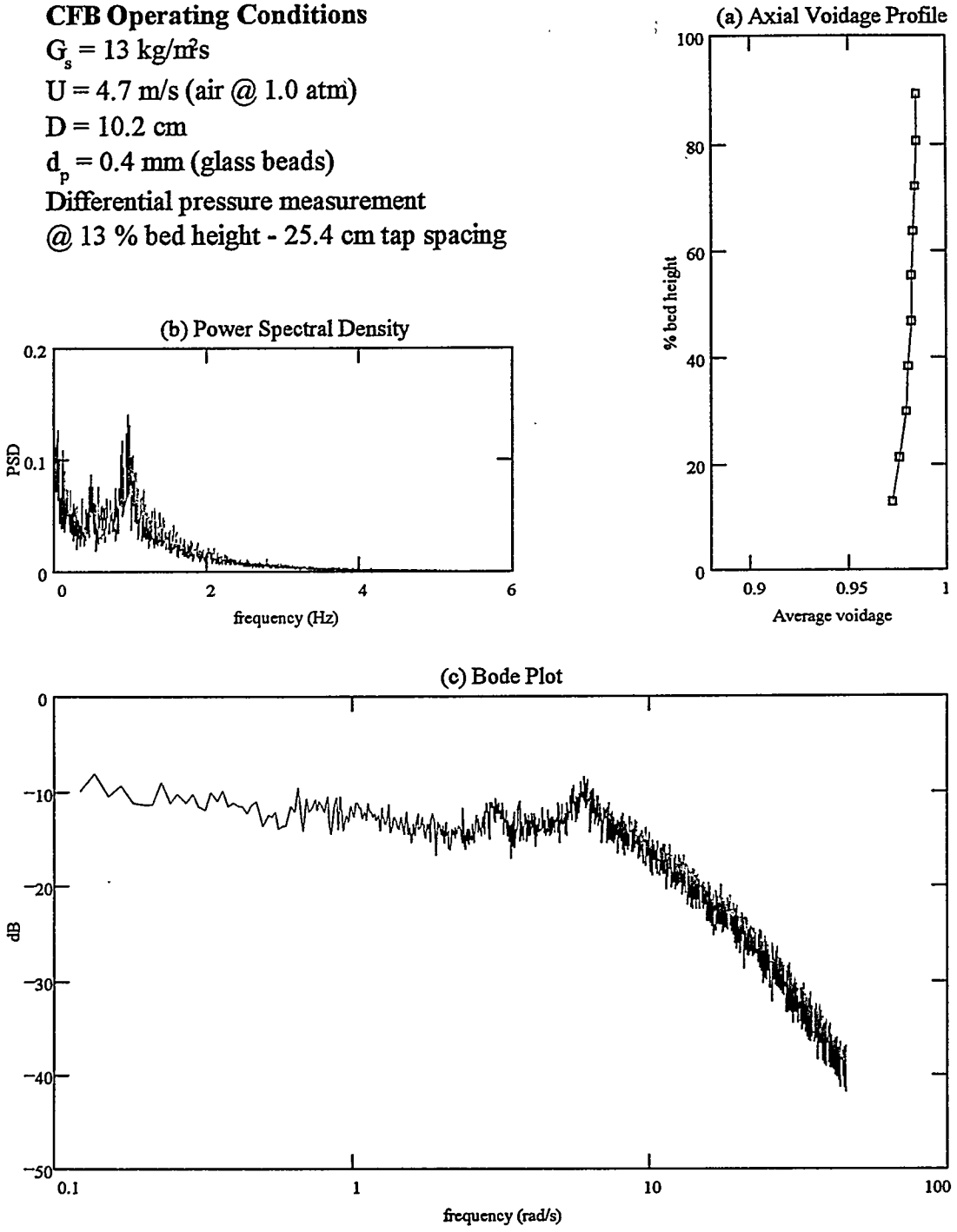

Figure 3: Dilute CFB operating conditions - a) axial voidage, b) PSD, c) Bode plot

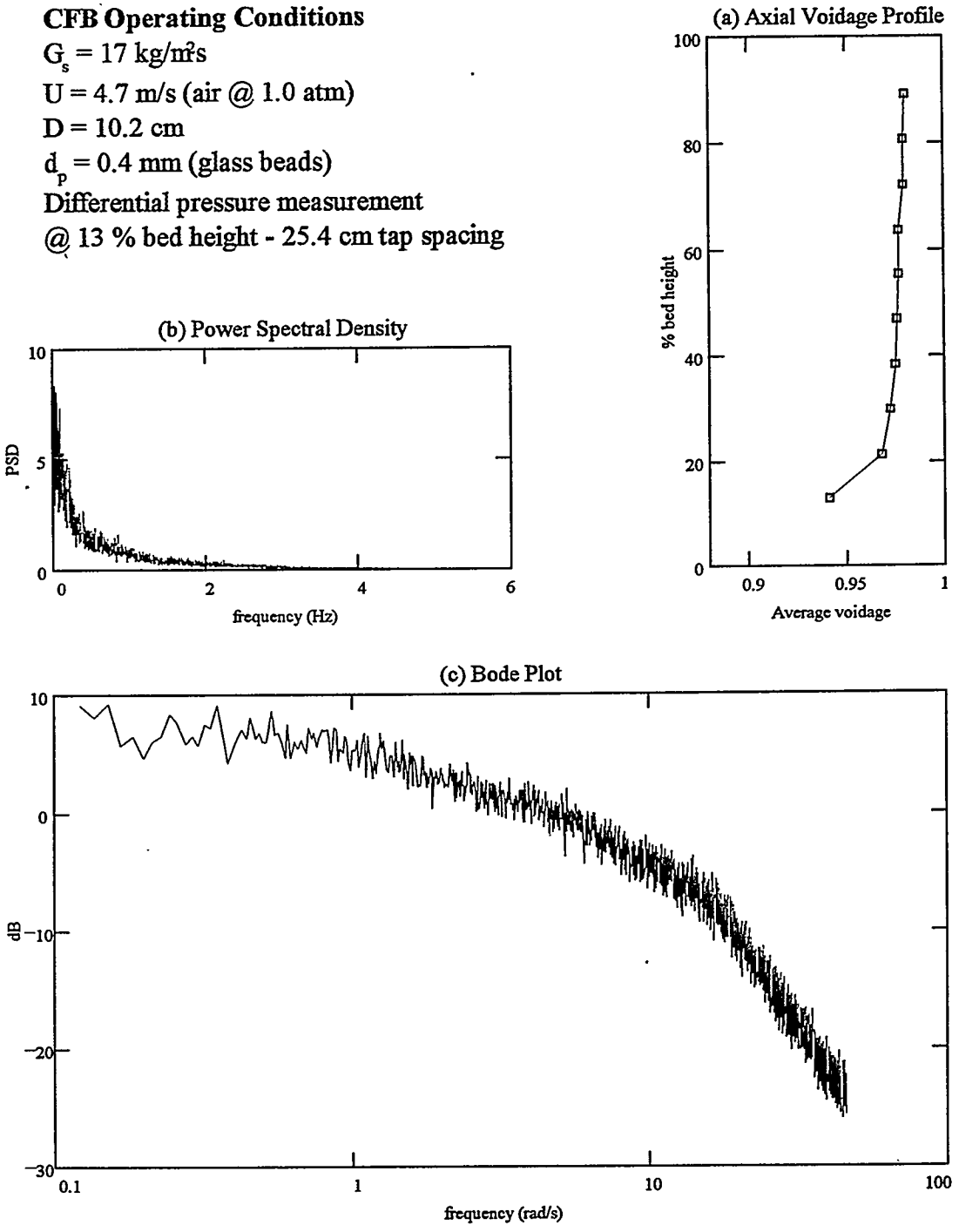

Figure 4: Damped CFB operating conditions - a) axial voidage, b) PSD, c) Bode plot

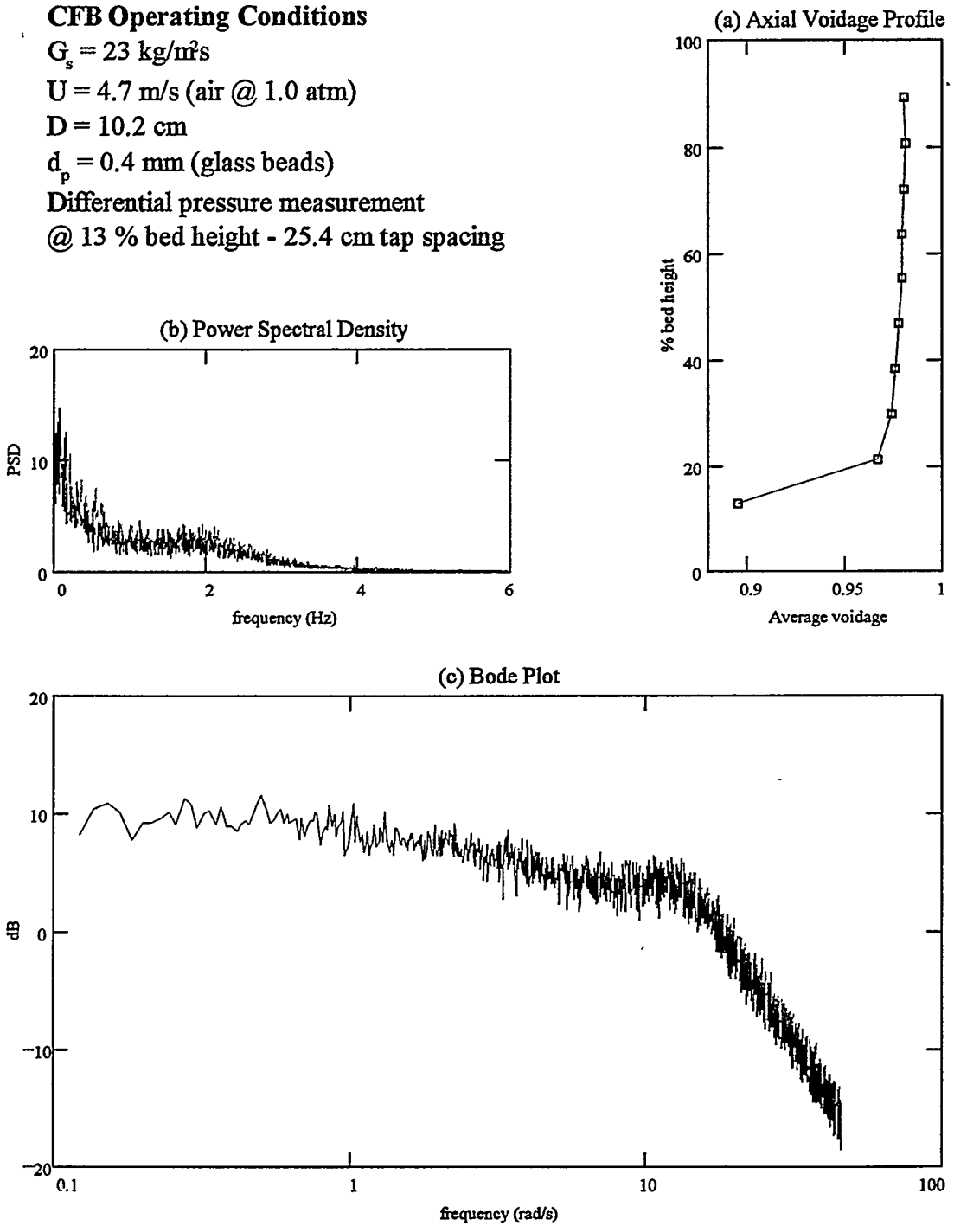

Figure 5: Dense CFB operating conditions - a) axial voidage, b) PSD, c) Bode plot

CFB Operating conditions:

$U = 4.1 \pm 0.2$ m/s (air @ 1.0 atm)
$G_s = 18 \pm 4$ kg/m^{2}s
$D = 10.2$ cm
$d_p = 0.3$ mm (glass beads)

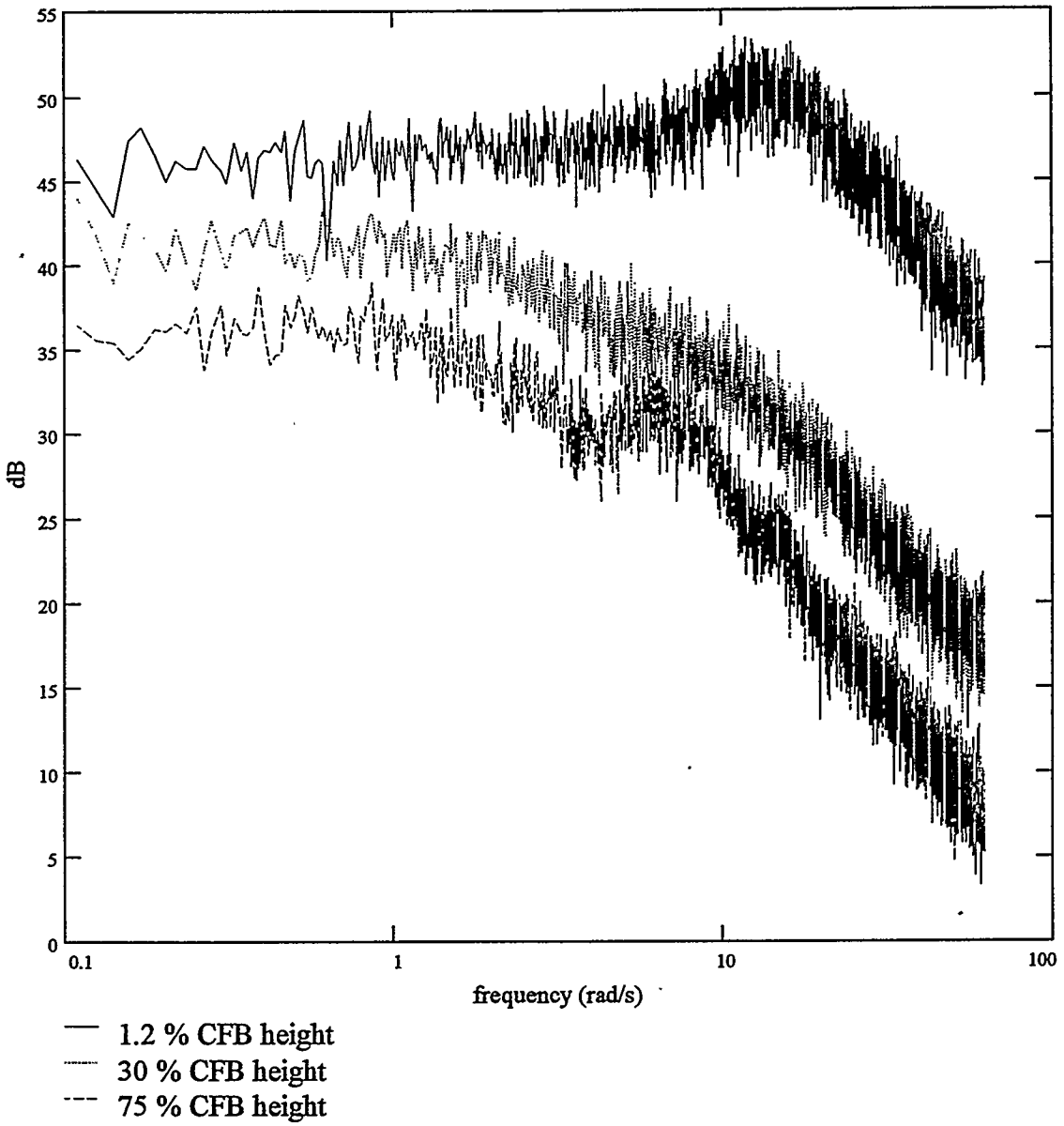

Figure 6: Appearance of dense phase phenomena at various bed elevations

Table 1. Summary of CFB similitude tests using Glicksman's parameters

Dependent parameters compared:
AVP - axial voidage profiles
5 % - Bode plots from 5 % total bed height
21 % - Bode plots from 21 % total bed height
75 % - Bode plots from 75 % total bed height

#	H/dp ($x10^{-4}$)	D/dp ($x10^{-2}$)	ρ_f/ρ_s ($x10^4$)	Re_p	Fr ($x10^{-3}$)	$G_s/\rho_s U$ ($x10^3$)	$M/\rho_s D^3$	AVP	5 %	21 %	75 %
1	1.5	5.1	4.7	40	4.6	1.3	2.1	*	no	*	**
2	1.5	5.1	4.7	40	4.6	1.9	2.1	*	no	no	*
3	1.5	5.1	4.7	47	6.3	1.7	2.1	no	no	*	*
4	1.5	5.1	4.7	47	6.3	2.1	2.1	no	no	no	**
5	1.5	5.1	4.7	47	6.3	2.8	2.7	*	no	*	**
6	1.5	5.1	4.7	54	8.2	1.9	2.1	no	*	*	*
7	1.5	5.1	4.7	54	8.2	2.4	2.7	*	no	no	*
8	1.1	3.4	4.7	71	4.2	1.1	2.1	no	no	no	*
9	1.1	3.4	4.7	71	4.2	1.7	2.1	NP	NP	NP	NP
10	1.1	3.4	4.7	81	5.4	1.4	2.1	no	no	no	*
11	1.1	3.4	4.7	81	5.4	1.9	2.7	no	no	no	*
12	1.1	3.4	4.7	81	5.4	2.4	2.1	NP	NP	NP	NP
13	1.1	3.4	4.7	110	11	1.4	2.1	no	no	*	**
14	1.1	3.4	4.7	110	11	1.7	2.7	no	no	*	**
15	0.8	2.5	4.7	108	4.1	1.0	2.1	no	no	no	**
16	0.8	2.5	4.7	108	4.1	1.4	2.1	NP	NP	NP	NP
17	0.8	2.5	4.7	126	5.6	1.2	2.1	no	no	**	**
18	0.8	2.5	4.7	126	5.6	1.6	2.7	*	no	*	**
19	0.8	2.5	4.7	148	7.7	1.4	2.1	no	*	*	**
20	0.8	2.5	4.7	148	7.7	1.7	2.7	no	no	*	**

Rating system:

** Bode plots match well in both models
* Not all Bode plot characteristics are similar in prototype and model
no Bode plots are not similar in prototype and model
NP Experiment *not possible* since chosen similitude parameters resulted in choking conditions in the protoype

Table 2. Operating conditions for similitude experiments (Figs. 7-11) Using riser loading as the independent solids parameter

SMALL CFB

L_v	23 ± 1 inches
Reactor loading	750 ± 25 mL
Superficial velocity	2.9 ± 0.1 m/s
Solids flux	30 ± 4 kg/m^{2}s
Rep	85 ± 12
Fr	5700 ± 800
$G_s/\rho_s U$	0.0014 ± 0.0002
H/d_p	10200 ± 1400
D/d_p	340 ± 50
ρ_g/ρ_s	2150 ± 30
$M/\rho_s D^3$	3.15 ± 0.08

LARGE CFB

L_v	45 ± 2 inches
Reactor loading	6000 ± 200 mL
Superficial velocity	4.1 ± 0.1 m/s
Solids flux	10 ± 2 kg/m^{2}s
Rep	84 ± 5
Fr	5800 ± 500
$G_s/\rho_s U$	0.0009 ± 0.0002
H/d_p	10200 ± 300
D/d_p	340 ± 10
ρ_g/ρ_s	2150 ± 70
$M/\rho_s D^3$	3.15 ± 0.05

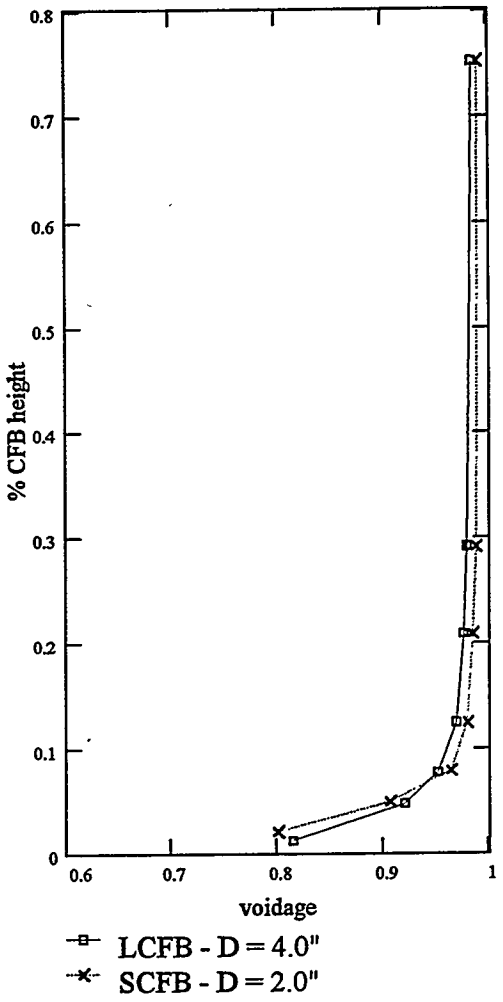

Figure 7: CFB axial voidage profiles (Using revised similitude parameters)

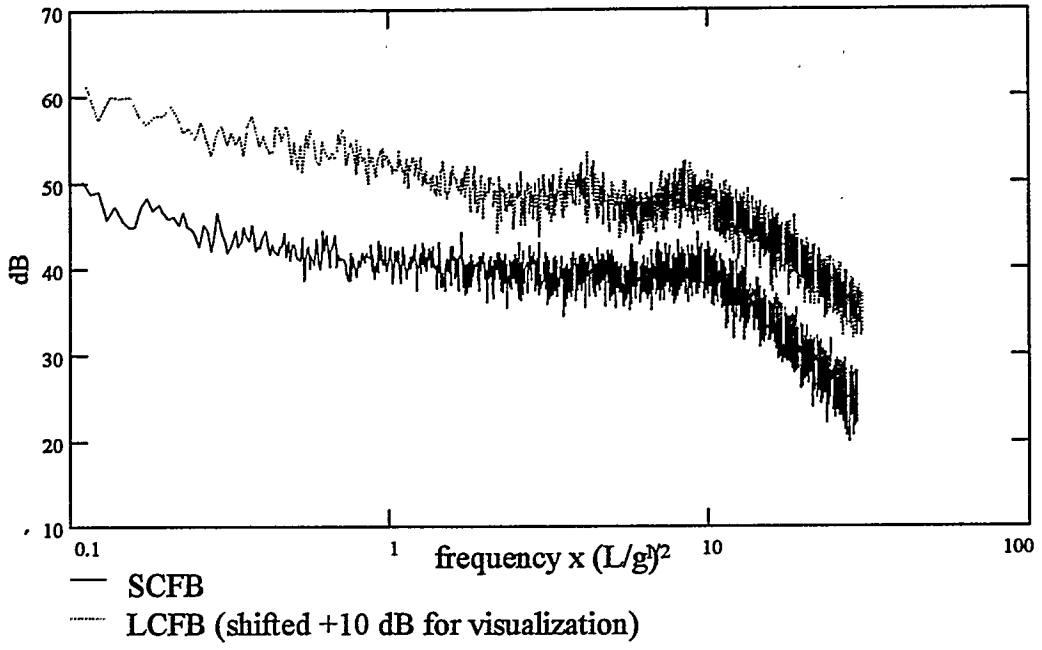

Figure 8: Bode plots of CFB under similitude conditions (1-2 % bed height) Using revised similitude parameters

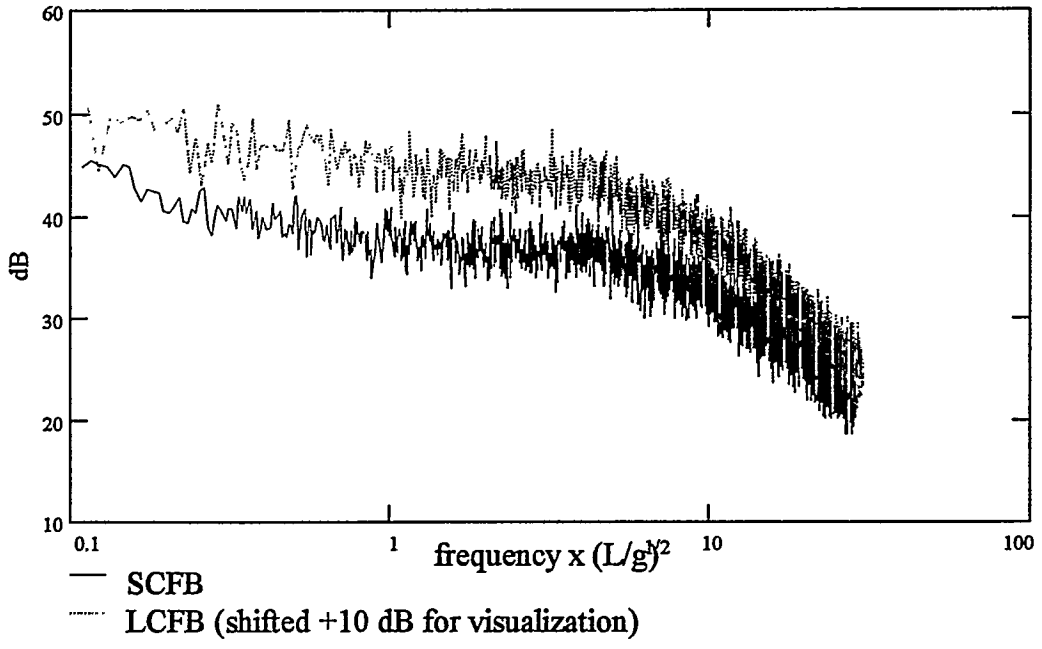

Figure 9: Bode plots of CFB under similitude conditions (5 % bed height) Using revised similitude parameters

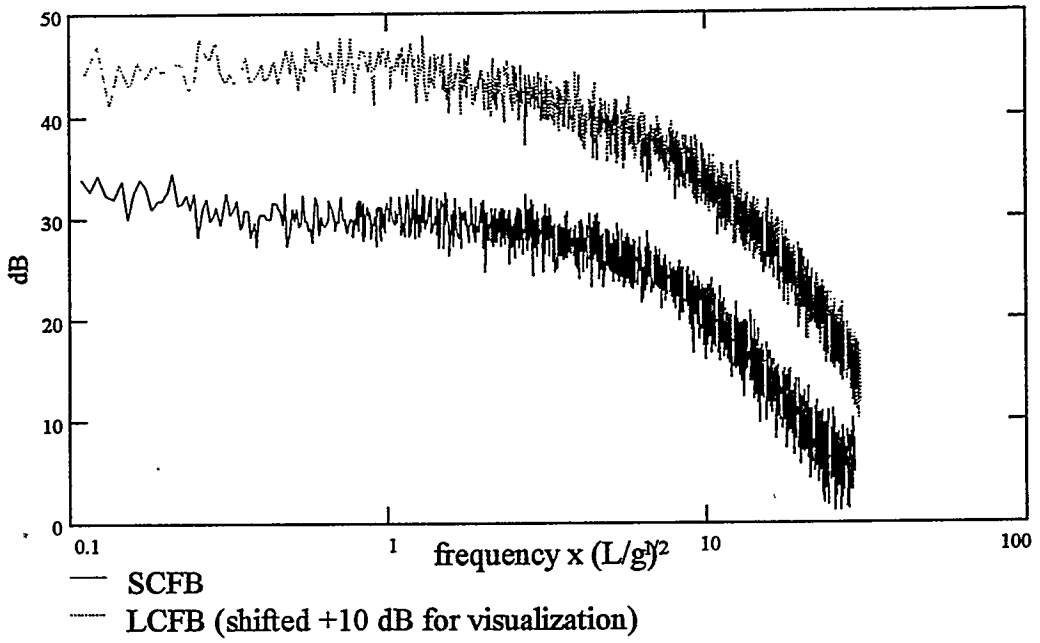

Figure 10: Bode plots of CFB under similitude conditions (13 % bed height) Using revised similitude parameters

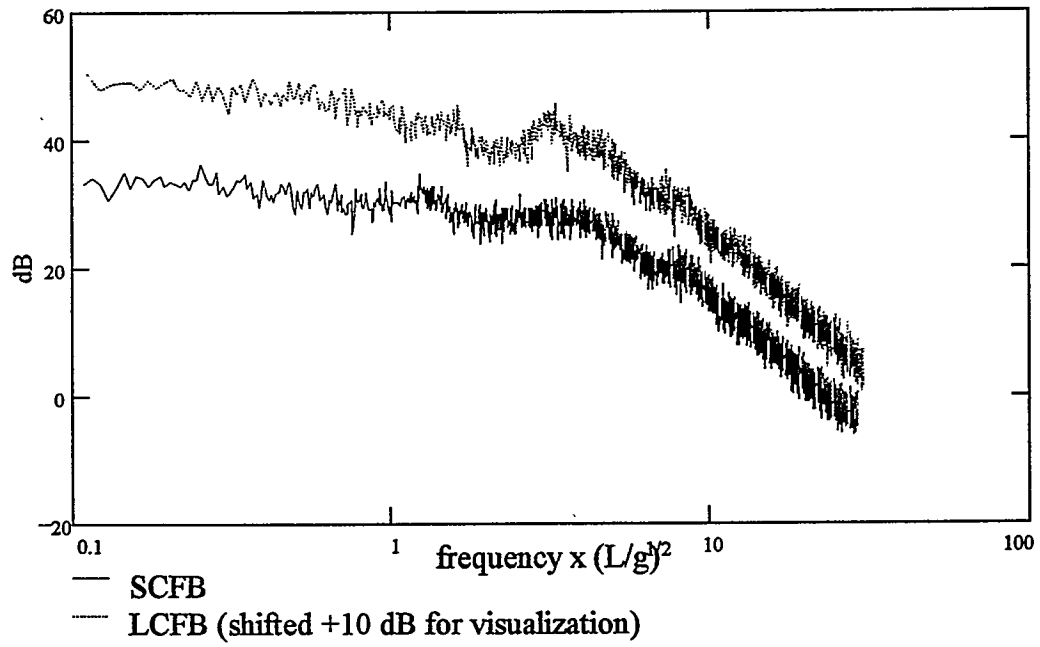

Figure 11: Bode plots of CFB under similitude conditions (75 % bed height) Using revised similitude parameters

Table 3 Operating conditions for similitude experiments (Figs. 12-16) Using riser loading as the independent solids parameter

SMALL CFB

L_v	16 ± 2 inches
Reactor loading	750 ± 25 mL
Superficial velocity	3.2 ± 0.1 m/s
Solids flux	35 ± 2 kg/m^{2}s
Rep	95 ± 13
Fr	7000 ± 1000
$G_s/\rho_s U$	0.0014 ± 0.0002
H/d_p	10200 ± 1400
D/d_p	340 ± 50
ρ_g/ρ_s	2150 ± 30
$M/\rho_s D^3$	3.15 ± 0.08

LARGE CFB

L_v	32 ± 1 inches
Reactor loading	6000 ± 200 mL
Superficial velocity	4.5 ± 0.1 m/s
Solids flux	13 ± 5 kg/m^{2}s
Rep	92 ± 5
Fr	7000 ± 500
$G_s/\rho_s U$	0.0010 ± 0.0004
H/d_p	10200 ± 300
D/d_p	340 ± 10
ρ_g/ρ_s	2150 ± 70
$M/\rho_s D^3$	3.15 ± 0.05

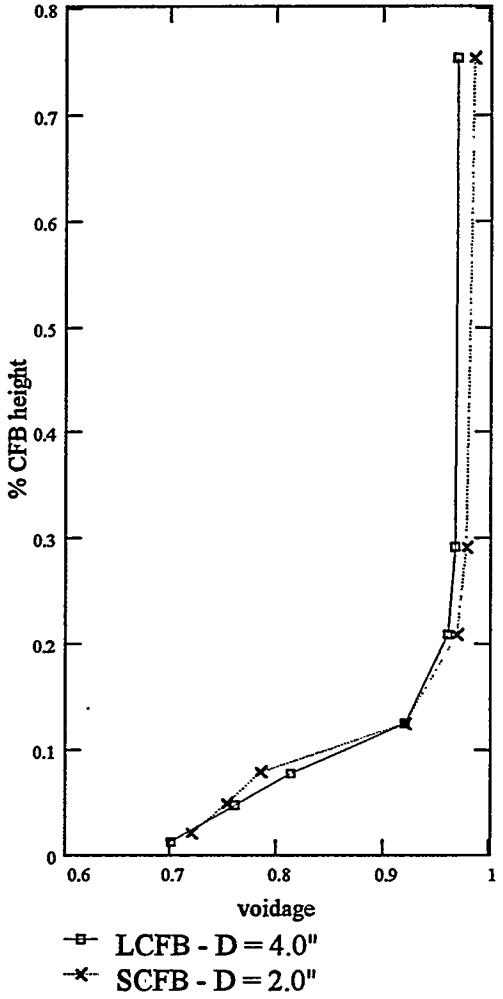

Figure 12: CFB axial voidage profiles (Using revised similitude parameters)

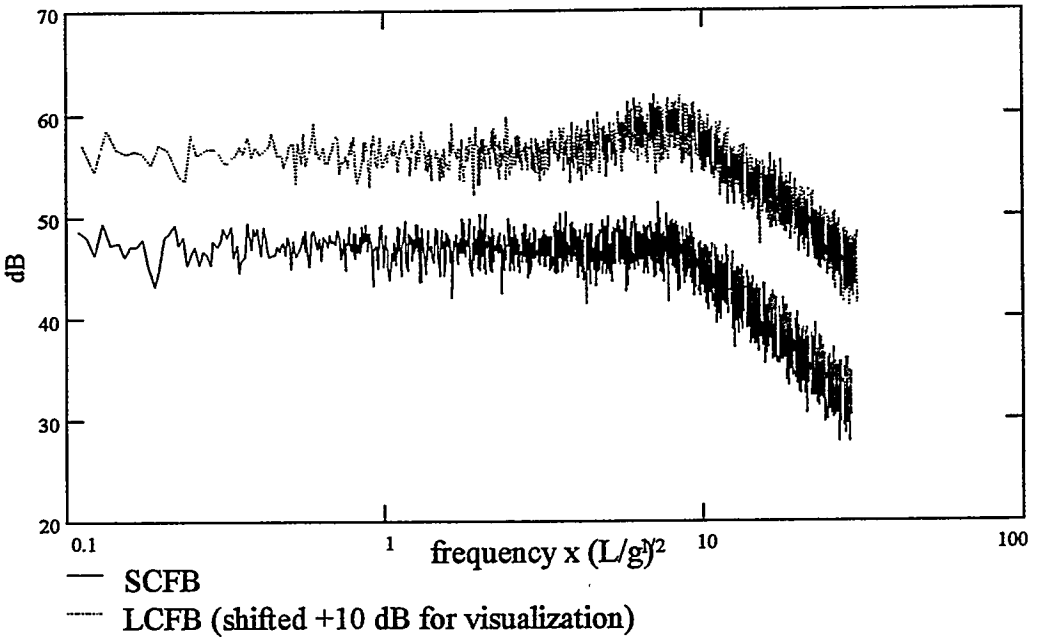

Figure 13: Bode plots of CFB under similitude conditions (1-2 % bed height) Using revised similitude parameters

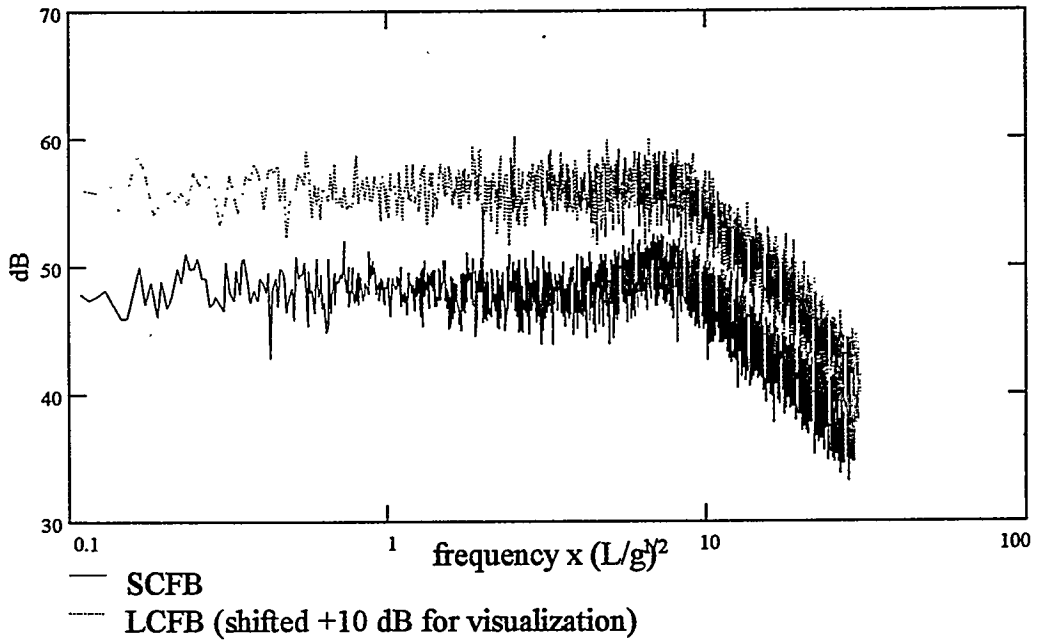

Figure 14: Bode plots of CFB under similitude conditions (5 % bed height) Using revised similitude parameters

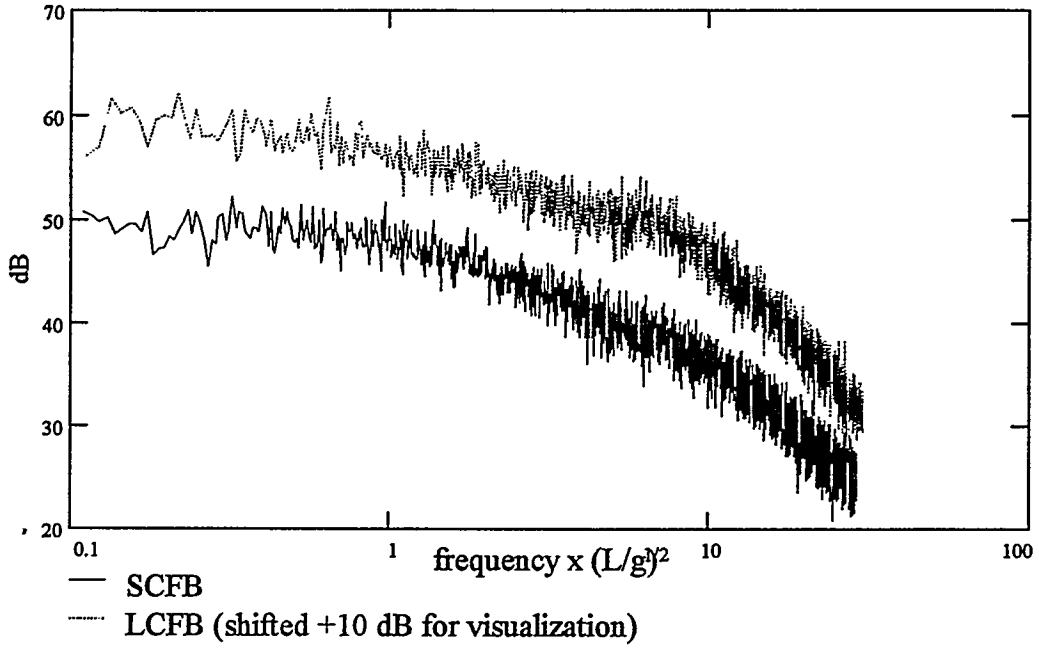

Figure 15: Bode plots of CFB under similitude conditions (13 % bed height) Using revised similitude parameters

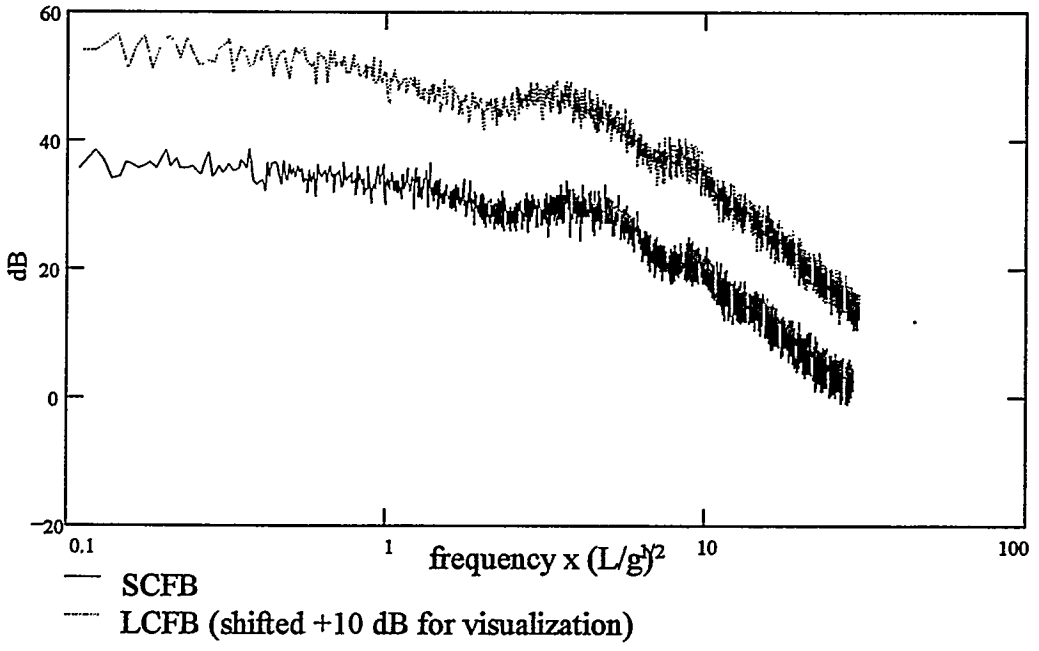

Figure 16: Bode plots of CFB under similitude conditions (75 % bed height) Using revised similitude parameters

Table 4. Operating conditions for similitude experiments (Figs. 17-21) Using dead-space extensions

SMALL CFB

L_v	23 ± 1 inches
Reactor loading	750 ± 25 mL
Superficial velocity	2.9 ± 0.1 m/s
Solids flux	22 ± 3 kg/m^{2}s
Rep	85 ± 12
Fr	5700 ± 800
$G_s/\rho_s U$	0.0010 ± 0.0001
H/d_p	10200 ± 1400
D/d_p	340 ± 50
ρ_g/ρ_s	2150 ± 30
$M/\rho_s D^3$	3.15 ± 0.08

LARGE CFB

L_v	46 ± 2 inches
Reactor loading	6000 ± 200 mL
Superficial velocity	4.1 ± 0.1 m/s
Solids flux	11 ± 2 kg/m^{2}s
Rep	84 ± 5
Fr	5800 ± 500
$G_s/\rho_s U$	0.0010 ± 0.0002
H/d_p	10200 ± 300
D/d_p	340 ± 10
ρ_g/ρ_s	2150 ± 70
$M/\rho_s D^3$	3.15 ± 0.05

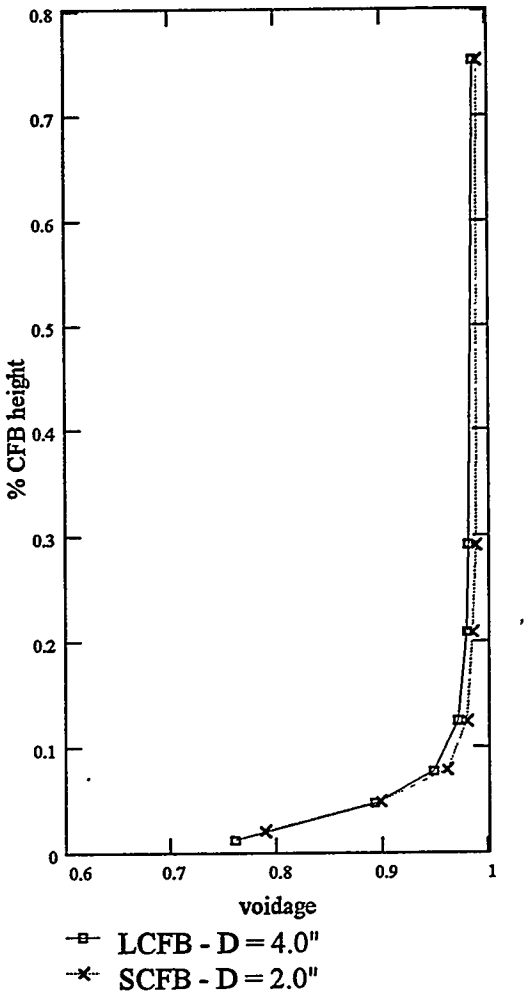

Figure 17: CFB axial voidage profiles (Using dead-space extensions)

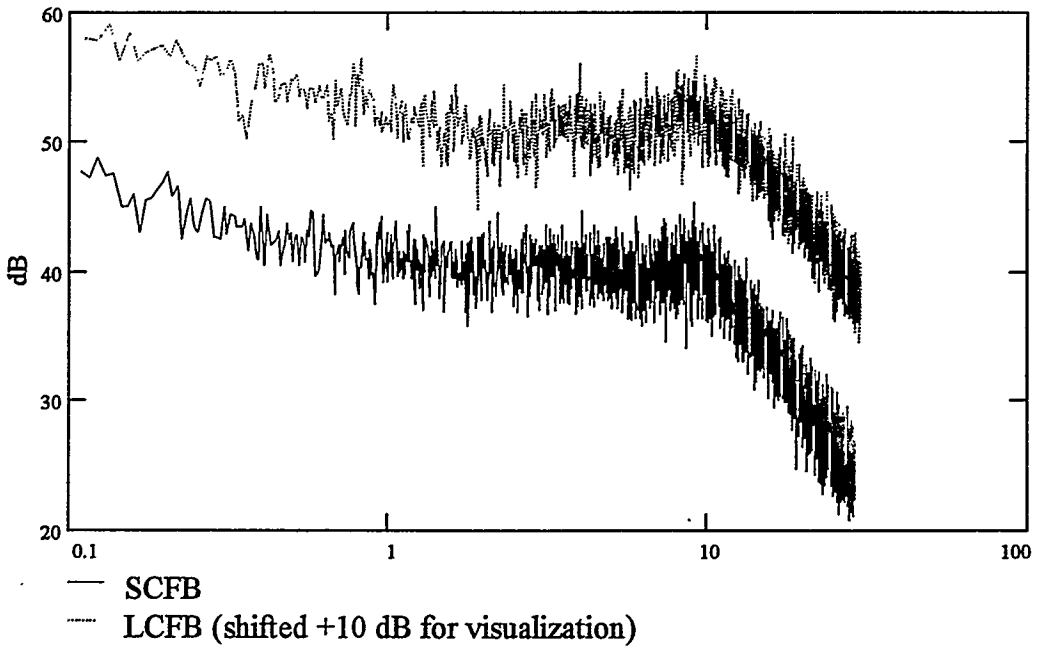

Figure 18: Bode plots of CFB under similitude conditions (1-2 % bed height) Using dead-space extensions

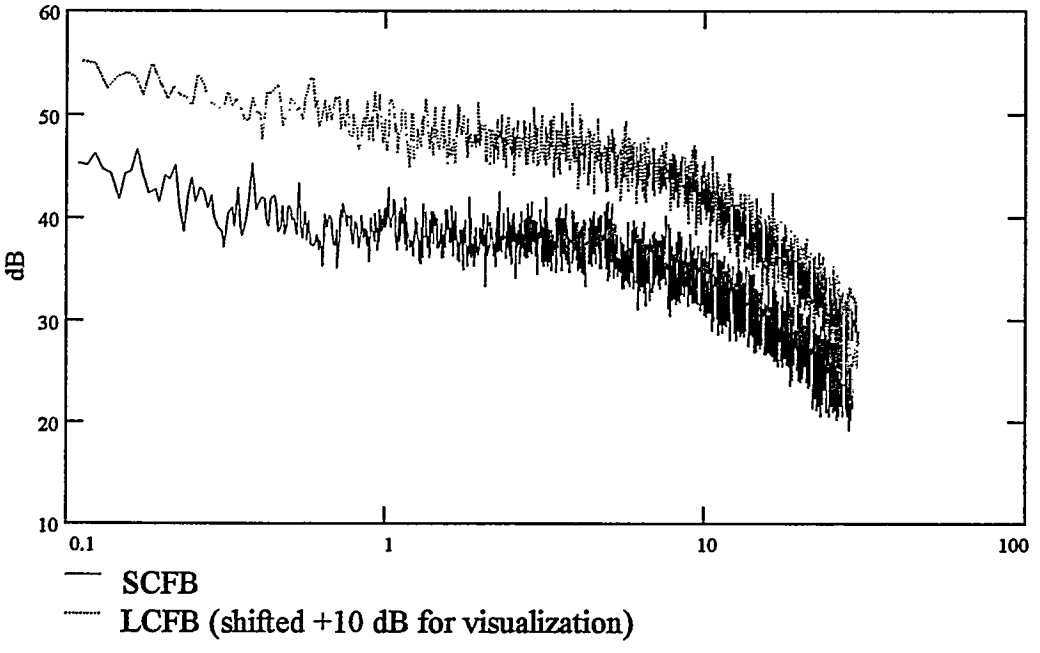

Figure 19: Bode plots of CFB under similitude conditions (5 % bed height) Using dead-space extensions

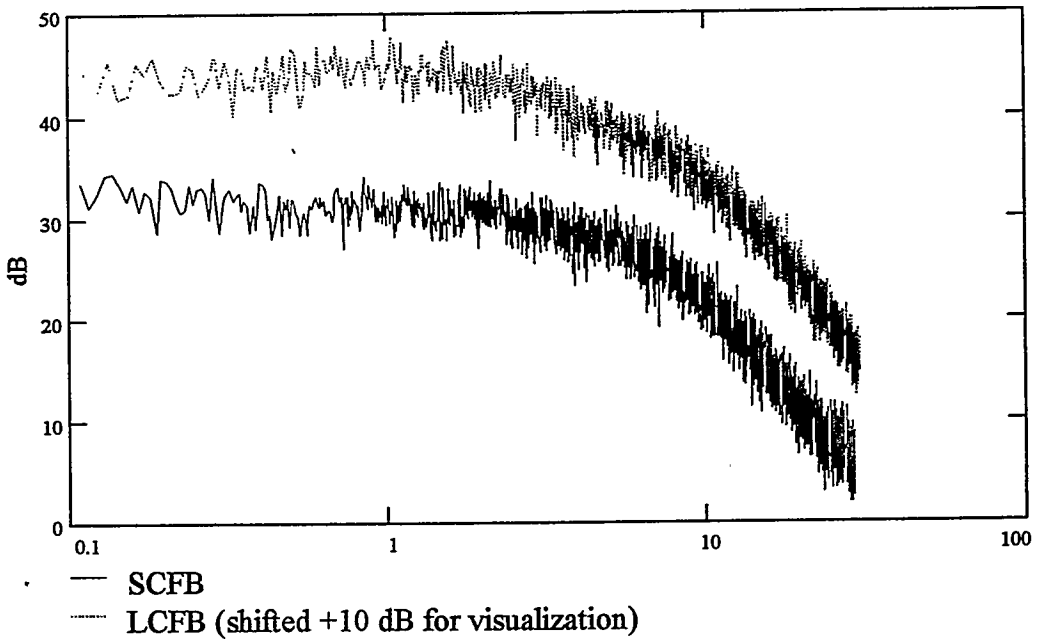

Figure 20: Bode plots of CFB under similitude conditions (13 % bed height) Using dead-space extensions

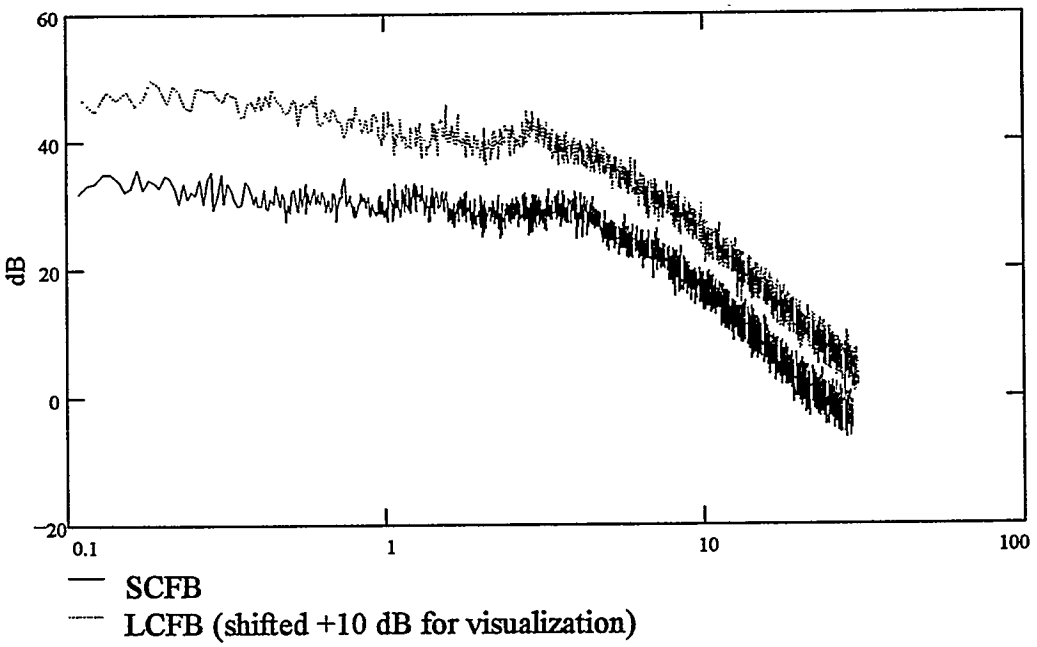

Figure 21: Bode plots of CFB under similitude conditions (75 % bed height) Using dead-space extensions